

# Optimal Charging of Electric Vehicles in Low-Voltage Distribution Systems

Peter Richardson, *Student Member, IEEE*, Damian Flynn, *Member, IEEE*, and Andrew Keane, *Member, IEEE*

**Abstract**—Advances in the development of electric vehicles, along with policy incentives, will see a wider uptake of this technology in the transport sector in future years. However, the widespread adoption of electric vehicles could lead to adverse effects on the power system, especially for existing distribution networks. These effects would include excessive voltage drops and overloading of network components, which occur mainly during periods of simultaneous charging of large numbers of electric vehicles. This paper demonstrates how controlling the rate at which electric vehicles charge can lead to better utilization of existing networks. A technique based on linear programming is employed, which determines the optimal charging rate for each electric vehicle in order to maximize the total power that can be delivered to the vehicles while operating within network limits. The technique is tested on a section of residential distribution network. Results show that, by controlling the charging rate of individual vehicles, high penetrations can be accommodated on existing residential networks with little or no need for upgrading network infrastructure.

**Index Terms**—Linear programming, load flow analysis, optimization methods, power distribution, road vehicle electric propulsion.

## I. INTRODUCTION

**E**LECTRIC vehicle technology is seen by many countries as a key component in the effort to reduce harmful greenhouse gas emissions, while also reducing the dependence on imported petroleum within the transport sector. As a result, many automotive manufacturers have begun to place increased emphasis on the development of various types of electric vehicles (EVs). These include battery electric vehicles, which operate purely from battery power, and plug-in hybrid electric vehicles, which operate on power from a combination of an on-board battery and a combustion engine. The batteries for both technologies can be recharged from external energy sources, e.g., an electricity network. Ambitious targets and incentives for introducing EVs into the transport sector have been proposed in

many countries [1]–[3]. Such targets, along with the likely increase in the cost of fossil fuels over the coming years, will see EV technology become more widespread.

Distribution networks are rated (kVA limit) to deliver electricity depending on the number of customers in a given area and the historical electricity demand data for each of those customers. The widespread adoption of EVs will introduce new customer demand patterns, and large vehicle penetrations could result in adverse effects on the network. Investigations into the potential impact of EVs on load patterns and the need for load management at the distribution network level have been conducted since as early as the 1980s [4], [5]. More recent work in this area has sought to investigate the limitations from large numbers of EVs on network infrastructure in terms of increased loading, impacts on efficiency, and loss of life for network assets [6]–[10]. These studies examined varying scenarios, such as unrestricted charging, peak and off-peak charging, diversified charging, and charging at varying power levels. The general consensus from these studies is that existing distribution networks should be able to accommodate substantial penetration levels of EVs if the majority of charging is restricted to low charging rates at off-peak times. Uncoordinated charging, especially fast, three-phase charging, will lead to an increase in the number of occurrences of component overloading and excessive voltage deviations if it coincides with existing peaks from the residential load. Staggering the charging start times for localized groups of EVs is also shown to help avoid these adverse effects, as well as spikes in demand due to simultaneous commencement of charging. The impact on voltage levels from high penetrations of EVs is also investigated in [11] and shows how high levels of coincident charging can cause voltages to drop beyond acceptable limits during times of high residential demand.

The introduction of advanced metering infrastructure (AMI) systems in residential housing, be it for real-time pricing or active demand side management, or both, will aid the control/predictability of the load patterns on residential networks. AMI could potentially have the ability to control certain loads within the household (including EVs) and allow DSOs or demand side aggregators to manage these loads in a coordinated manner. Such concepts have been investigated previously. The work described in [12] proposes management strategies for EV charging/discharging in LV microgrids. By allowing network control devices to respond to voltage and frequency levels, it is shown that the EV load can enable LV microgrids to be operated in a stable manner. In [13], a technique is employed to minimize power losses and on-load tap changes for the network transformer, mainly due to the charging/discharging of EVs located far from the slack bus.

Manuscript received November 17, 2010; revised March 08, 2011 and April 29, 2011; accepted May 23, 2011. Date of publication June 23, 2011; date of current version January 20, 2012. This work was conducted in the Electricity Research Centre, University College Dublin, Ireland, which is supported by the Commission for Energy Regulation, Bord Gáis Energy, Bord na Móna Energy, Cylon Controls, EirGrid, the Electric Power Research Institute (EPRI), ESB Energy International, ESB Energy Solutions, ESB Networks, Gaelectric, Siemens, SSE Renewables, SWS Energy, and Viridian Power & Energy. This publication has emanated from research conducted with the financial support of Science Foundation Ireland under Grant Number 06/CP/E005. Paper no. TPWRS-00923-2010.

The authors are with the School of Electrical, Electronic, and Mechanical Engineering, University College Dublin, Dublin, Ireland (e-mail: peter.richardson@ucd.ie; damian.flynn@ucd.ie; andrew.keane@ucd.ie).

Digital Object Identifier 10.1109/TPWRS.2011.2158247

In [14], various techniques are utilized to investigate the impact of varying penetrations of EVs on residential networks. Quadratic and dynamic programming techniques minimize the impact from EV charging on network losses and voltage deviation in particular. By controlling and optimizing individual EV charging rates, network losses and voltage deviations are reduced for all penetration levels examined. The methodology is examined using both deterministic and stochastic methods and concludes that while the difference in the results obtained using the quadratic or dynamic technique is negligible, the dynamic technique is more computationally intense. Work in [15] investigated the use of voltage control on EVs with charge/discharge capabilities. Here the objective was to minimize the charging cost to the EV owner while maintaining network voltage levels within acceptable limits. Results were shown to vary significantly depending on the initial state of charge of the EV batteries, with high dependence on the tariffs associated with charging and discharging.

The work in this paper differs in its approach to the coordinated charging of EVs described above. Instead of minimizing power losses and/or voltage deviations, the objective of the optimization technique employed here is to maximize the total amount of energy that can be delivered to all EVs over a charging period while ensuring that network limits are never exceeded due to high levels of coincident EV charging. Such an approach ensures that optimal use is made of available network capacity while avoiding excessive voltage drop and component overloading, which have been shown, in work cited above, to be potential issues with high levels of EV charging. The technique employs linear programming that takes advantage of the approximately linear characteristics of both the network voltages and component loading sensitivities to the addition of EV load.

The methodology for this work is presented in Section II. Section III describes the modeling of the test network, the residential load, and the electricity demand profiles of EVs. Results and discussion for two specific charging periods are presented in Section IV along with generalized results for a wide range of network scenarios. Conclusions are presented in Section V.

## II. METHODOLOGY

### A. Assumptions

Coordinated charging of EVs could be achieved in a variety of ways. It is assumed here that EV owners are incentivized to charge their vehicles at off-peak times of day. Once the off-peak period has begun, no additional EVs will connect for charging and no EVs will disconnect before reaching a full battery state of charge (BSOC). Smart metering technology with load control capability is also assumed to be present in each household. It is assumed that this load control capability can be utilized by the DSO (or a third-party aggregator), from a remote location, in order to manage certain loads on the consumer side of the meter. Such a scheme would be subject to prior agreement by both the consumer and the DSO. For the purposes of this work, the ability to control the load extends to EV charging only and allows the operator to vary the charging rate of each EV on the

feeder. Each EV can charge at any rate between zero and the maximum rated output, subject to certain restrictions, which are outlined later in this section. The ability to vary the charge rate of individual EVs in a continuous manner has been studied for use in optimal charging strategies previously [14], [16], [17]. While the possibility exists for fast, three-phase charging, it is assumed that each EV will be connected to the network via a standard single-phase AC connection. Although the concept of vehicle-to-grid for local system support or otherwise exists [12], [13], [15], [17], bi-directional flow of electricity to and from an EV battery is not considered in this work.

### B. Standard Objective Function

The objective of the method is to maximize the energy delivered to all EVs within a set period of time. This is achieved by optimizing the charging rate of each connected EV in order to maximize the total power that can be delivered for each 15-min time interval, subject to network constraints. Coordinating the charging of EVs ensures that the network is utilized to its fullest extent in terms of energy delivered.

The standard objective function,  $F$ , is given as

$$F = \sum_{i=1}^N P_{EV_i} x_i \quad (1)$$

where  $N$  is the number of customers being served by the network, and  $P_{EV_i}$  is the power delivered, measured in kW, to the EV connected at the  $i$ th customer point of connection (CPOC). It is assumed that  $P_{EV_i}$  is a continuous control variable that can vary between 0 kW and the maximum power output of the charger at node  $i$ .  $x_i$  is zero when an EV is not connected at the  $i$ th CPOC or the EV battery is fully charged, while  $x_i$  equals one when the EV at the  $i$ th CPOC is connected and the EV battery is less than fully charged.

### C. Constraints

At each time step, the objective function,  $F$ , is maximized subject to certain constraints. The first of these is that the power demand of an EV cannot exceed the rated power output of the charger supplying that vehicle, (2):

$$0 \leq P_{EV_i} \leq P_{EV_i}^{\max}. \quad (2)$$

In order to avoid large variations in the charging rate over consecutive time steps, which is undesirable for current battery technology [18], a rate of change constraint is also imposed (3):

$$P_{EV_i}^{t-1} - \Delta \leq P_{EV_i}^t \leq P_{EV_i}^{t-1} + \Delta. \quad (3)$$

Here,  $t$  is the current time step and  $\Delta$  is a defined limit, in kW, by which the charging rate can vary, compared to the charging rate at the previous time step, excluding on/off transitions.

The next constraint relates to the acceptable voltage range for the LV network. The addition of EV loads, for the most part, will cause the voltage at various points of the network to drop. The extent of the voltage drop can vary depending on a number of factors, which include the location of the EV and the rate of

charge. The voltage at each CPOC must be maintained within the rated voltage range specified for the network, (4):

$$V_{\min_i} \leq V_i \leq V_{\max_i} \quad \forall N. \quad (4)$$

Here,  $V_i$  (V) is the voltage at the  $i$ th CPOC, while  $V_{\min_i}$  and  $V_{\max_i}$  are the minimum and maximum allowable network voltage levels, respectively.

The thermal loading of network components refers to the ratio of the apparent power flowing through the component to its rated capacity. For this study, the thermal loading of both the network transformer and the mains cable connecting the transformer to the network are considered. These constraints are summarized in (5) and (6), respectively:

$$L_{TX} \leq L_{TX_{\max}} \quad (5)$$

$$L_{MC} \leq L_{MC_{\max}} \quad (6)$$

where  $L_{TX}$  and  $L_{MC}$  are the thermal loading (kVA) for the transformer and mains cable, respectively, while  $L_{TX_{\max}}$  and  $L_{MC_{\max}}$  are the associated maximum loading of the components.

#### D. Network Sensitivities

A time-series, unbalanced, three-phase load flow analysis of the test network is performed in order to determine the network voltage and thermal loading levels as a result of the residential household load. This is performed using power system analysis software [19] and applying residential load information. The voltage sensitivities at each CPOC are also calculated for both the addition of EV load at their own terminal and at each of the other household terminals on the network, i.e., the change in voltage due to charging demand from the EVs. For each time step, EV load is added incrementally at each CPOC in turn and the change in voltage at each CPOC is recorded. This data is then used to calculate the voltage sensitivities of the network to the addition of EV load. The addition of EV load to any CPOC on the network causes variations in the voltage at each of the other CPOCs. Thermal loading sensitivities for the network components of interest are calculated in the same manner. The addition of EV load at any point of the network causes an increase in the thermal loading experienced by the transformer. Analysis of the load flow results shows that the assumption of linearity for both the voltage and thermal loading sensitivity characteristics is adequate [11]. The constraint for the voltage level can be summarized as

$$V_{\min_i} \leq V_{init_i} + \mu_i P_{EV_i} + \sum_{j=1}^N \mu_{ji} P_{EV_j} \leq V_{\max_i} \quad \forall N, \quad i \neq j \quad (7)$$

where  $V_{init_i}$  is the initial voltage at the  $i$ th CPOC of the network with no EVs charging,  $\mu_i$  (V/kW) is the sensitivity of the voltage at the  $i$ th CPOC due to power demanded by the EV connected at the same CPOC, and  $\mu_{ji}$  is the sensitivity of the voltage at the  $i$ th CPOC due to power demanded by an EV connected at the  $j$ th CPOC.

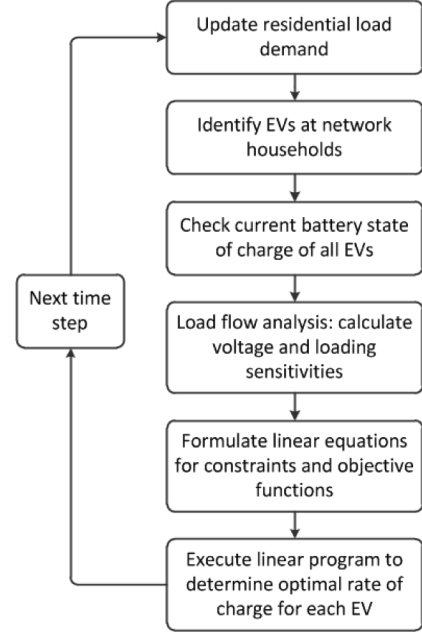


Fig. 1. Methodology for optimizing the charging rates of EVs.

The thermal loading constraints are summarized as

$$L_{TX_{init}} + \sum_{k=1}^N \delta_k P_{EV_k} \leq L_{TX_{\max}} \quad \forall N \quad (8)$$

$$L_{MC_{init}} + \sum_{k=1}^N \beta_k P_{EV_k} \leq L_{MC_{\max}} \quad \forall N \quad (9)$$

where  $L_{TX_{init}}$  and  $L_{MC_{init}}$  are the initial thermal loading levels of the network transformer and mains cable, respectively, and  $\delta_k$  (kVA/kW) and  $\beta_k$  (kVA/kW) are the sensitivities of the transformer and mains cable loading to power demand ( $P_{EV_k}$ ) of an EV at the  $k$ th CPOC.

The voltage and thermal loading sensitivities are determined for each time step of the analysis. Subsequently, a linear programming tool in [20] determines the optimal charging rate for each connected EV for each time step, in order to maximize the total amount of energy that can be delivered over the considered period. A summary of the methodology is outlined in the flow chart presented in Fig. 1.

#### E. Weighted Objective Function

Due to the radial layout of the majority of LV residential networks, the standard optimization technique tends to charge EVs connected near to the transformer at a higher rate than those located far from the transformer. This is due to the voltage levels being less sensitive to the addition of EV load near to the transformer. In order to provide a more even distribution of energy to the charging EVs and prioritize batteries with a low BSOC, a modified objective function is applied to the optimization algorithm, which applies a weighting according to each individual EV's BSOC at the previous time step. It is assumed that the BSOC of each EV is known at the beginning of each optimization time step. The modified objective function,  $F$ , is summarized as follows:

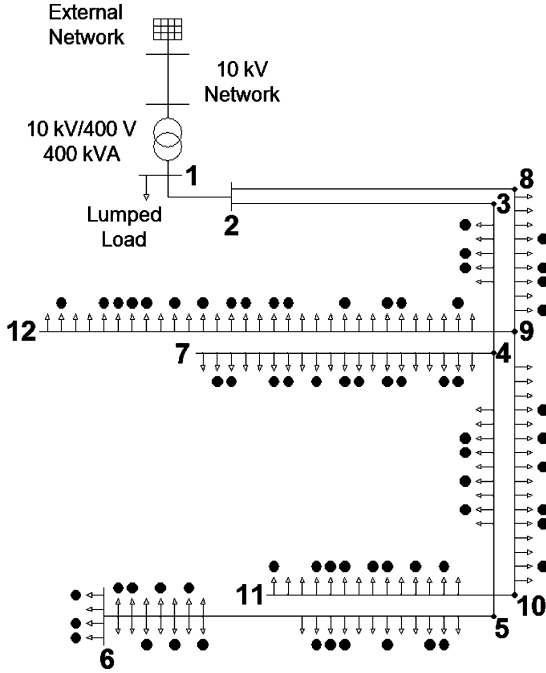


Fig. 2. Single line diagram of test network. Circles show houses where EVs are connected for charging.

$$F = \sum_{i=1}^N \left( 1 - \left( \frac{\text{BSOC}_i}{\text{BSOC}_{\max_i}} \right) \right) P_{\text{EV}_i} x_i \quad (10)$$

where  $\text{BSOC}_i$  is the current battery state of charge (kWh) of the EV connected at the  $i$ th CPOC and  $\text{BSOC}_{\max_i}$  is the maximum battery capacity of that EV.

### III. MODELING OF TEST NETWORK

#### A. Distribution Network

The test network is based on an LV residential distribution feeder in a suburban area of Dublin, Ireland. A simplified representation of the feeder is given in Fig. 2. In the actual test feeder, each household, EV, and service cable are modeled separately. The model incorporates a 400 kVA, 10/0.4 kV step-down transformer supplying a feeder of 134 residential customers through 1.2 km of three-phase copper mains cables and 980 m of single-phase copper service cables. A lumped load model, representing a similar number of residential customer loads with no EV loads, is included to represent another feeder being supplied from the same transformer.

In Ireland, the LV distribution network is operated at a nominal voltage of 230/400 V with a voltage range tolerance of  $\pm 10\%$  [21]. For the most part, LV substation transformers in Ireland do not have tap-changing capabilities, which is the case for the transformer modeled in the test network. As such, the medium voltage (MV) network supplying the LV transformer is included in the model as an equivalent impedance in order to take account of the voltage drop at this network level. The MV network is modeled such that at maximum residential load (with no EV charging), the voltage at all points of the network does

not exceed  $-10\%$  of nominal. Specifications for the network model components were supplied by Electricity Supply Board (ESB) Networks, who are the DSO in the Republic of Ireland, and are given in Table III in the Appendix.

#### B. Residential Customer Load Modeling

Typical load data for domestic electricity demand customers was obtained from the DSO consisting of 15-min time-series demand data for high, medium, and low use customers over a one-year period. Different electricity demand profiles were randomly assigned to each of the houses in the test network. However, in order to confirm that these load profiles portrayed an accurate representation of the power demanded by a real distribution feeder, the coincidence factor of the test network was determined. The coincidence factor is defined as the ratio of the maximum diversified demand divided by the maximum non-coincidental demand [22]. From assessing the yearly load profiles for each of the households on the network, the coincidence factor was found to be 0.32, which compares favorably with similar residential networks [23].

For modeling purposes, the power factor for each household load is set at 0.97 inductive during the day and 0.95 inductive at night. Here, daytime is specified as between 6 am and 10 pm, and nighttime as between 10 pm and 6 am. The load is modeled as a combination of constant power (P) and constant impedance (Z). From April to September inclusive, the load is modeled as 60% constant P, 40% constant Z. From October to March inclusive, the load is modeled as 40% constant P and 60% constant Z, due to an increase in electric heating load. It is common practice to model residential loads in this manner when exact information on the load type is not available [23].

#### C. Electric Vehicle Load Modelling

It is assumed that each EV is connected at the same CPOC as the household load through a single-phase connection. Charging profiles for EVs can vary depending on battery type, charging equipment, and the electricity supply network. For this work, EV batteries are modeled based on lithium-ion battery technology. It is assumed that once connected, an individual EV with no charge controlling capability charges at a rate of 4 kW up to a BSOC of approximately 95%. After this point, the vehicle charges at a rate of 1.5 kW until the battery has reached its maximum capacity. For this work, all EV batteries are modeled with a capacity of 20 kWh. The EV charging equipment is assumed to have a 90% efficiency rating. The charging rate of 4 kW is appropriate in terms of the power delivery capabilities of existing LV distribution networks in Ireland [21]. EV batteries are modeled as constant power loads with unity power factor.

#### D. Time Periods for Investigation

In order to demonstrate the benefits of the optimization technique, two specific periods of time within the one year period of residential load data were chosen. For this study, the charging period occurs from 10 pm to 7 am the next day. One test period was chosen because it contained the highest 15-minute residential demand during the off-peak charging periods (winter scenario). The maximum 15-minute residential demand for this

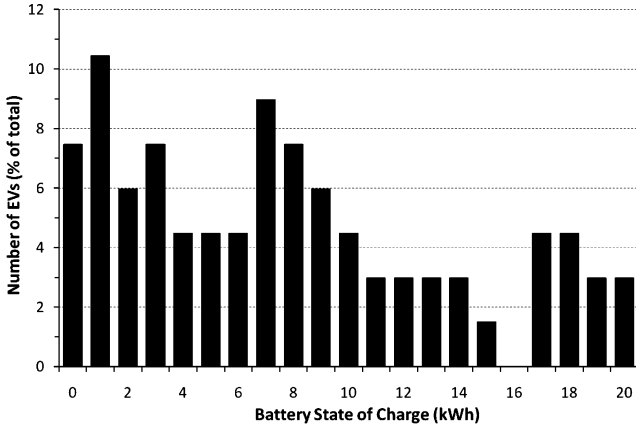


Fig. 3. Distribution of the initial BSOC for each EV.

TABLE I  
INITIAL EV CONDITIONS

	Number of EVs	Combined Battery Capacity (kWh)	Combined Initial BSOC (kWh)	Total Energy Required (kWh)
Phase a	19	380	139	241
Phase b	18	360	146	234
Phase c	30	600	236	344
Total	67	1340	521	819

time period was approximately 152 kW. The other test period chosen was a low-demand mid-week charging period in the summer (summer scenario).

For the simulations, half of the residential households were randomly assigned an EV, as shown in Fig. 2. This amounts to 67 EVs on the network with a potential combined maximum demand of 268 kW. It was assumed that all EVs remain connected to the network for the entire charging period, with each EV randomly assigned an initial integer valued BSOC. The distribution of the initial BSOC for each EV is shown in Fig. 3. The average initial BSOC of all the EVs was 7.8 kWh, or 39% of the maximum BSOC.

Table I shows the breakdown of EVs allocated to the network as well as the total energy requirement of these vehicles on a phase-by-phase basis. It is clear from this table that there is a greater number of EVs on phase c, and thus a larger energy requirement, compared to the other phases. While a 50% penetration of EVs on a distribution feeder may not be experienced in reality for many years to come, it was deemed appropriate to examine such a demanding scenario in order to fully capture the main benefits from controlled charging strategies compared to uncontrolled charging.

#### E. Stochastic Scenario Analysis

The charging periods identified above are chosen to examine the optimization technique for specific network scenarios. However, in order to demonstrate the benefits of the optimization technique for a wider range of scenarios, a stochastic tool is developed to generate different residential load scenarios with

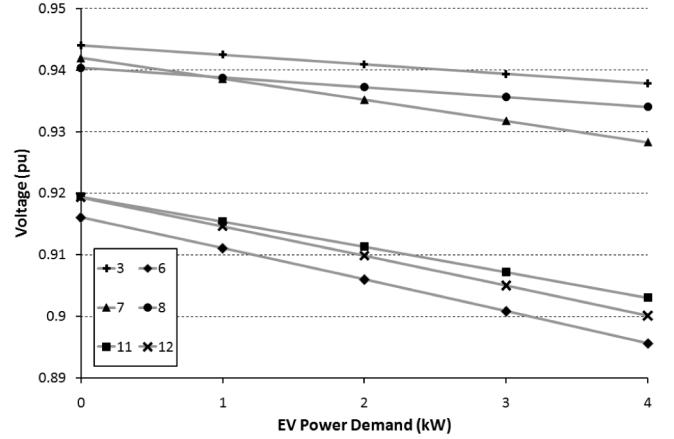


Fig. 4. CPOC voltage sensitivities to charging EVs at 6 network points for the Winter Scenario.

probabilistic conditions for varying residential load, EV location, and initial BSOC.

Probability distribution functions (PDFs) for the household load were created based on the residential load data provided by the DSO with PDFs for low, medium, and high use customers. Then, 15-min household load profiles were generated for each house for a 9-h period from 10 pm to 7 am the next day, similar to the deterministic analysis. It is assumed that all EVs are connected for charging at the beginning of this period and remain connected until the end. At the beginning of each 9-h charging period the EV locations on the network were randomly selected with each one then assigned an initial BSOC. As no real charging data was available, a PDF (mean = 10.75 kWh, standard deviation = 6 kWh) for assigning initial BSOC was created. For each charging period time step, network sensitivities are determined which are then used to optimize the charging rate of each EV. The load model and power factor for both the residential and EV load remain the same as for the deterministic analysis.

## IV. RESULTS AND DISCUSSION

The optimization technique is tested with the two different objective functions, (1) and (10). The results for each approach are outlined below and are compared to scenarios with no EV charging present and with uncontrolled EV charging.

#### A. Network Sensitivities

For each 15-min time interval, a series of three-phase, unbalanced load flow calculations are performed using the customer demand profiles in order to determine the voltage and thermal loading sensitivities of the network due to the introduction of EVs. These sensitivities inform the optimal charging rate of each EV for each time step of the charging period. The voltage sensitivity at each CPOC is measured for varying charging rates and varying EV charging locations on the network. Fig. 4 demonstrates how the voltages measured at the CPOCs closer to the transformer (i.e., 3 and 8 from Fig. 2) are less sensitive to the addition of EV loads as compared to those located near the end of the feeder (i.e., points 6, 7, 11, and 12).

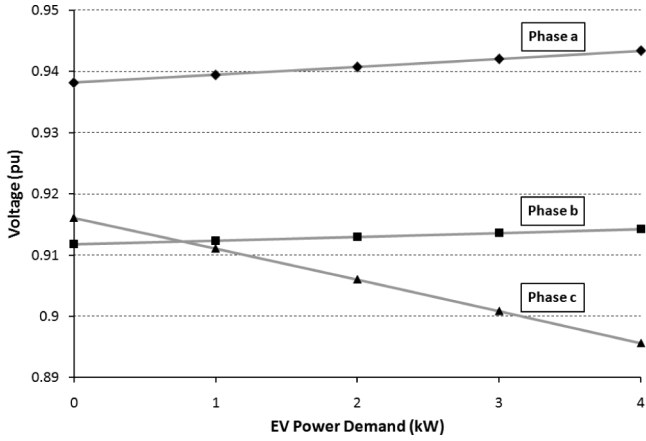


Fig. 5. Interdependence of 3 CPOC voltages with EV charging on phase c for the Winter Scenario.

Since the household loads for this network are connected to individual phases of the network, the addition of EV load to a particular CPOC affects the voltage at that particular CPOC as well as the voltage on the other phases of the network, as demonstrated in Fig. 5. As can be seen, the addition of EV load on phase c only causes the voltage on that phase to decrease while the remaining phase voltages increase slightly. This effect is not uncommon in unbalanced networks [22] and is captured in the voltage constraint equation, (7), where the sensitivity,  $\mu$ , of the voltage at a particular CPOC can be either positive or negative depending on the phase to which an EV is connected.

The voltage sensitivities can vary significantly due to the changes in the domestic household load, and therefore they are calculated for each time step of the analysis. This information is then subsequently used to optimize the EV charging rates, the results of which are outlined in Section V.

In order to determine the accuracy of the optimization technique, error margins were calculated based on the difference between the predicted CPOC voltages from the optimization algorithm and the CPOC voltages recorded from the subsequent load-flow calculations. The average maximum error margin over the summer charging period was found to be 1% for the standard and weighted objective functions. For the winter charging scenarios, these values were recorded as 1.4% (standard objective function) and 1.5% (weighted objective function). As can be seen in the results presented below, the accuracy of the sensitivities is adequate to ensure that no operating limits are exceeded due to EV charging.

### B. Uncontrolled EV Charging

With no active control over EV charging rates, all of the EVs would be expected to commence charging at the beginning of the charging time period at the maximum rate of charge. As the network is not rated for this high level of demand, the network operating conditions are severely impacted. Fig. 6 shows the voltage level at a CPOC at node 6 for the Winter Scenario base case. The charge profile for an EV connected at the same CPOC is also displayed. The initial BSOC of this EV was 3 kWh or 15%. While all EVs on the network would be fully charged by the end of the charging period, the lower voltage limit at this

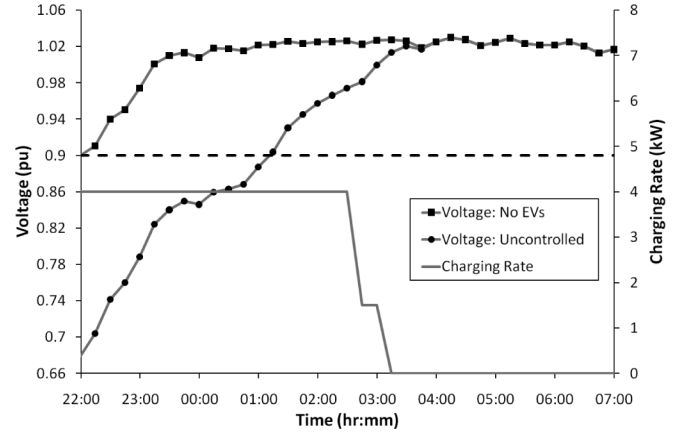


Fig. 6. Voltage level for a CPOC at node 6 for base case and uncontrolled charging scenarios with charge profile for an EV charging at the same CPOC (Winter Scenario).

CPOC, i.e., 0.9 pu, is exceeded for over 3 h at the start of the charging period. The lowest voltage experienced at this node is approximately 0.68 pu. It is clear that such a scenario could not be permitted to occur and it is likely that the number of EVs on the network would be restricted to a predetermined limit. For the purposes of comparison, an uncontrolled charging scenario was created whereby there is a limit to the number of EVs that are allowed to charge simultaneously. This number was determined by incrementally adding EVs, charging at the maximum rate of charge, to the extremities of the feeder up to the point before the feeder exceeds an allowable operating limit. This test was performed with the residential load at the maximum expected midnight demand. Charging was restricted to begin only after midnight to ensure that the residential load is off-peak. For the test network utilized in this work, the predetermined number of EVs that could be allowed to charge in an uncontrolled scenario was found to be 21.

### C. Controlled EV Charging

By employing the methodology described in Section II, the rate at which each EV charges is now optimized in order to deliver the maximum power to the EVs while maintaining all voltages and network flows within acceptable operating limits for each time step. At the beginning of the charging period, the total energy required to return all EVs to 100% BSOC is 819 kWh. For the optimization, the lower voltage limit is set at 210 V or 0.913 pu, which allows for a margin of safety with respect to the lower voltage limit defined in the Irish distribution network code [21]. This ensures that any unexpected short-term variations in the demand, will not cause the network to exceed its operating limits. The maximum variation allowable for the rate of charge between time steps, i.e.,  $\Delta$  in (3), is set at 0.25 kW for each of the control strategies.

1) *Standard Objective Function*: From Table II, it can be seen that using the standard objective function a total of 810 kWh in the summer and 798 kWh in the winter were delivered to the EVs by the end of the respective charging periods. Although this means that the total EV energy requirement (819 kWh) was not met, in both cases the network was maintained

TABLE II  
TOTAL ENERGY DELIVERED TO EV BATTERIES

		Total Energy Delivered (kWh)	% Energy Requirement
Uncontrolled Charging (21 of 67 EVs)	Summer	238	29
	Winter	238	29
Standard Objective Function	Summer	810	98.9
	Winter	798	97.4
Weighted Objective Function	Summer	818	99.9
	Winter	815	99.5

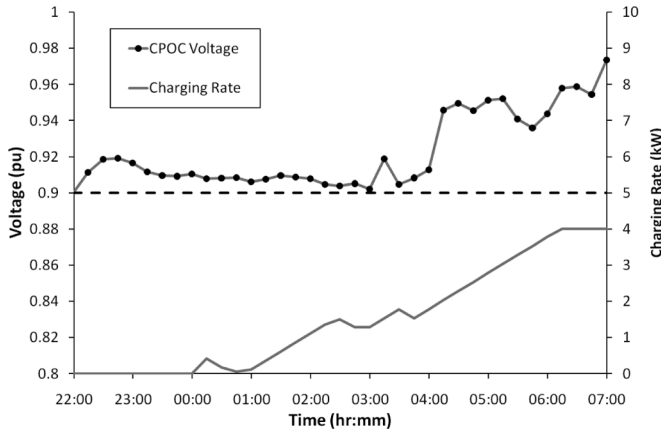


Fig. 7. Voltage profile for a CPOC at node 6 and charge profile for EV charging at the same CPOC with optimized charging employing the standard objective function (Winter Scenario).

within normal operating limits for the entire duration of the charging period.

The voltage profile of a CPOC at node 6 with an EV charging and the corresponding EV charge profile is given in Fig. 7. It is evident that the voltage here is a binding constraint for the optimization technique as it is held just above the lower voltage limit for the majority of the charging period. It can also be seen that the EV connected to this CPOC does not truly begin charging until the third hour of the charging period and does not approach a maximum rate of charge until towards the end of the period. This particular EV had an initial BSOC of 3 kWh (15%) and had reached a BSOC of 15 kWh (75%) by the end of the charging period. Clearly, this would be an unacceptable outcome for an EV owner that desired a full BSOC.

Fig. 8 shows the distribution function for the BSOC of each EV at the end of both the summer and winter charging periods. It is evident in both cases that a number of EVs, including the one shown in Fig. 7, have not reached a full BSOC by the end of the charging period. In the summer scenario, 64 of the 67 EVs were fully charged, while for the winter charging period, 63 EVs had a full BSOC. In both cases, the EVs with a BSOC of less than 100% are all located near the end of the branches of the feeder and are connected to phase c. From Table I, it can be seen that a greater number of EVs are connected to phase c than either of the other phases, which results in a larger energy requirement. Additional load due to EV charging at CPOCs near the end of feeder branches will have a greater effect on network voltage

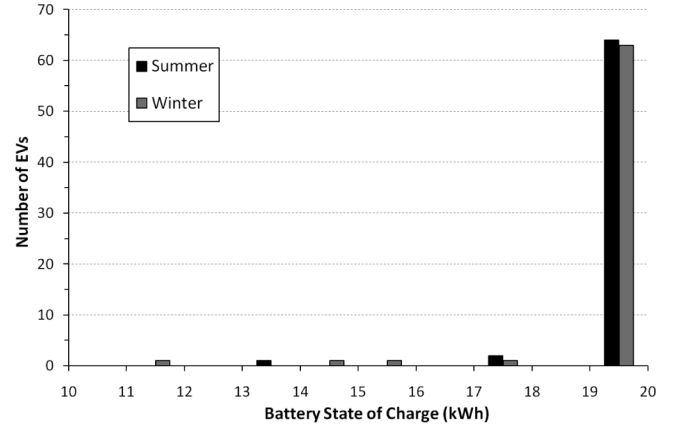


Fig. 8. Distribution function of the battery state of charge for all EVs at end of the summer and winter charging periods: standard objective function.

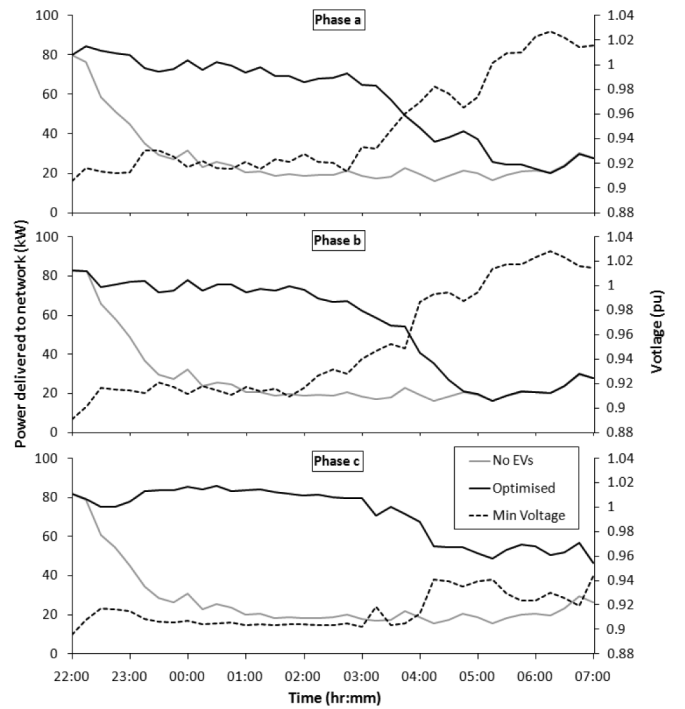


Fig. 9. Power delivered to network on each phase for the case with no EVs charging and the optimized charging case employing the standard objective function (Winter). The lowest CPOC voltage for each phase at each time step for the optimized charging case is also shown.

levels than if located closer to the transformer. As a result, the optimization method allocates low charging rates to these EVs until the other EVs are fully charged. The combination of both factors leads to a number of EVs not receiving a full BSOC by the end of the charging period. This outcome is displayed in Fig. 9, which shows the active power demand, with and without EV charging, on each phase of the network over the charging period. It is clear that, while the EVs connected to phase a and phase b have completed charging, power is still being delivered to some EVs connected to phase c. Also shown in this figure is the lowest CPOC voltage measured on each phase of the feeder for each time step. It is clear that while power is being delivered to the EVs on the feeder, the voltage levels at each of the CPOCs are held above the lower voltage limit.

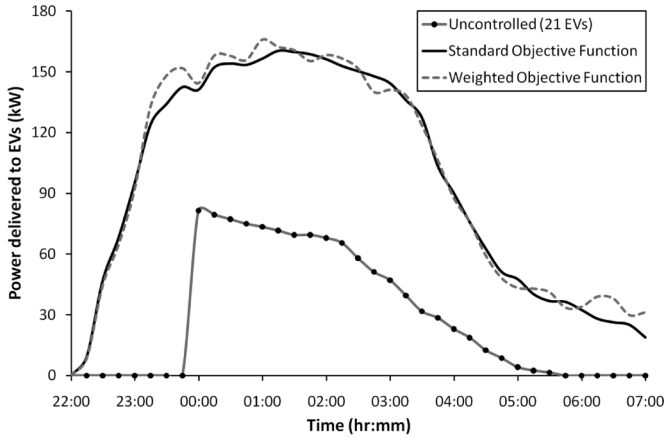


Fig. 10. Total power delivered to EVs for uncontrolled and optimized winter charging scenarios.

2) *Weighted Objective Function*: The standard objective function optimization technique will consistently tend to assign low charging rates to EVs located further from the transformer. Such a situation would clearly be unacceptable. In order to overcome this, the optimization process was repeated, as described in Section II, with the objective function weighted according to the current BSOC of each charging EV, (10).

By employing this method, 818 kWh of energy are delivered to the EVs for the summer charging period and 815 kWh are delivered in the winter charging period, which represents 99.9% and 99.5%, respectively, of the total energy required to return all EV batteries to a full BSOC. The total power delivered to the EVs for the uncontrolled and optimized charging scenarios is shown in Fig. 10. While both objective function methods deliver similar energy totals by the end of the charging period, the individual EV charging patterns vary significantly across the network. During the early stages of the charging period, the SOF prioritizes EVs that are located close to the transformer, whereas the WOF assigns higher charging rates to EVs with a low BSOC, wherever they may be located in the network. Later in the charging period, applying the SOF, vehicles located at the network extremes begin charging. As the voltage is more sensitive to additional load at these points of the network, the charging rates for these EVs are lower and less energy can be delivered. The same restrictions are not as severe using the WOF as the energy delivered to the EVs is more evenly distributed across the network, resulting in more energy being delivered towards the end of the charging period (Figs. 13 and 14).

Fig. 11 shows the voltage profile, for the same CPOC as shown in Fig. 7, as a result of the weighted objective function optimization technique. Once again, it is apparent that the voltage at this CPOC is a binding constraint. However, the EV begins charging much earlier and the BSOC by the end of the charging period has reached 100%, as compared with a figure of 75% using the standard objective function method.

The distribution function of the BSOC for the EVs by the end of the charging period is given in Fig. 12, and shows an increase in the number of EVs with a full BSOC for both charging period scenarios when compared to the previous method. Specifically,

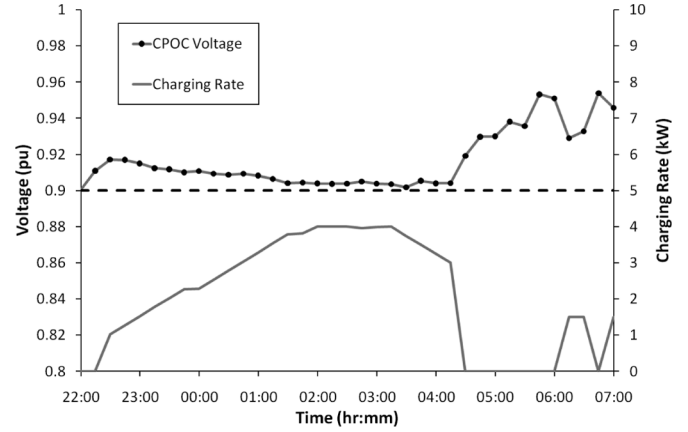


Fig. 11. Voltage profile for a CPOC at node 6 and charge profile for EV charging at the same CPOC with optimized charging employing the weighted objective function (Winter Scenario).

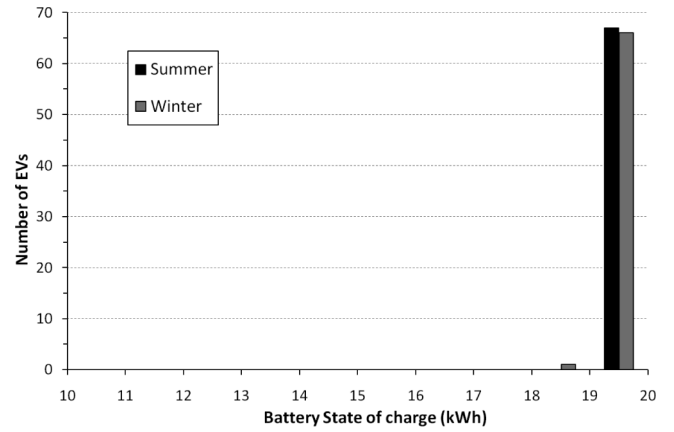


Fig. 12. Distribution function of the battery state of charge for all EVs at end of the summer and winter charging periods: weighted objective function.

67 EVs have a full BSOC by the end of the summer charge period, while 66 of the 67 EVs have a full BSOC in the winter scenario. This compares favorably to the standard objective function method where the lowest BSOC of all the EVs was 68% and 58% for the summer and winter charging periods, respectively. As was the case for the previous method, the EV that was not fully charged was connected to phase c and is located near the end of the feeder branches.

It should be noted that the particular allocation of EVs in this work resulted in there being a greater number of EVs connected to one phase compared to the others. As this work has shown, even an optimal method for maximizing the energy that can be delivered to charging EVs may be insufficient if a large number of the EVs are connected to the same phase of the network at the same time. Such scenarios may require that the DSO reconfigure the distribution of load across the phases.

#### D. Thermal Loading of Network Components

Thermal loading constraints of certain feeder components are also taken into account by the optimization technique. Fig. 13 shows the loading of the LV transformer over the charging period for the Winter Scenario, while Fig. 14 shows the loading for the three-phase mains cable (Line 1–2 in Fig. 2) that supplies



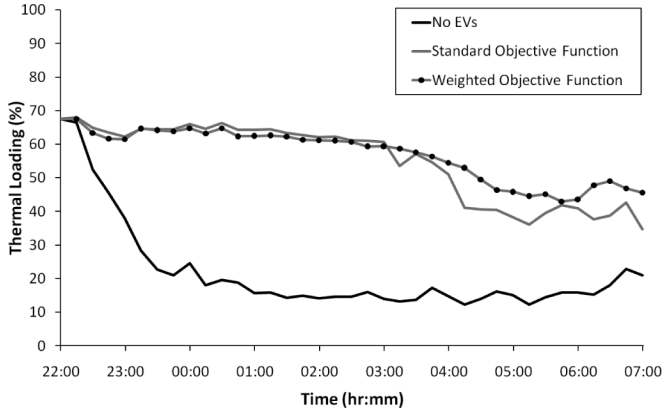


Fig. 13. Thermal loading of LV transformer for winter charging period.

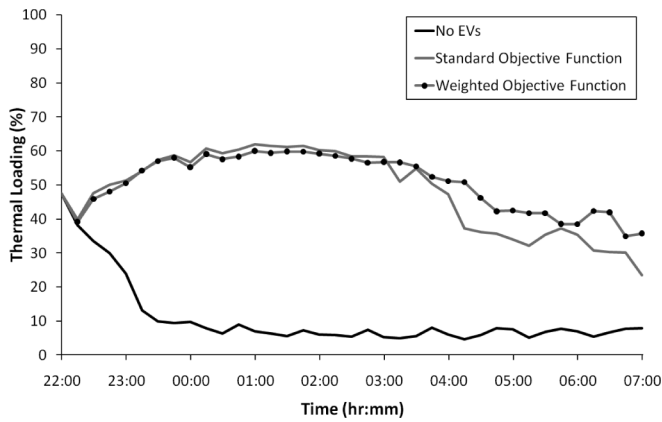


Fig. 14. Thermal loading of three-phase mains cable supplying feeder for winter charging period.

the feeder from the transformer for the same scenario. In both cases, it is evident that neither the transformer nor the mains cable loading are the binding constraint on this network. Clearly, the network equipment is more than adequately rated for accommodating the additional load that would be demanded by this high penetration of EVs, assuming that the majority of charging occurs at off-peak times of day. This may not be the case for all residential distribution feeders, many of which may experience overloading of network components due to large numbers of EVs charging simultaneously at both peak and off-peak times of day. Without some form of controlled charging for EVs, a significant increase in the number of overloading incidences will impact on the lifetime of these network components [6]. By employing a controlled charging technique, like the one described in this paper, the overloading of network components due to EV charging can be avoided by incorporating certain constraints, (8) and (9). While this would result in increased loading levels during the off-peak period, a flatter transformer load profile would impact less on the transformer lifetime than a profile with large overloads due to on-peak EV charging [24]. Together with the introduction of other demand side management schemes, many forms of residential load could be controlled in a manner which would allow networks to be utilized to their fullest extent while not impacting on component lifetimes.

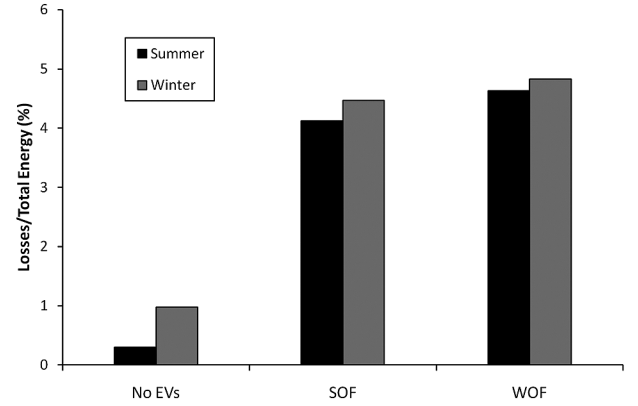


Fig. 15. Network losses for standard objective function (SOF) and weighted objective function (WOF) cases.

### E. Network Losses

The network losses as a percentage of the total energy delivered to the network are presented in Fig. 15. For each of the cases studied, the losses ratio is greater in the winter charging period than in the summer period due to the increased residential demand in the winter. The added demand from EVs charging causes the losses ratio to increase significantly. This is evident for both the standard (SOF) and weighted (WOF) objective function methods. For the SOF case the losses ratio increases from 0.3% to 4.1% in the summer and 1% to 4.5% in the winter. For the WOF method, these values increase to 4.6% in the summer and to 4.8% in the winter scenario.

### F. Stochastic Scenario Analysis

A stochastic analysis of the network loading is carried out in order to provide insight into the effects of the optimization technique while accounting for the variability associated with a high penetration of charging EVs. The optimization technique using the weighted objective function was simulated for 500, 9-h charging periods (i.e., 18 500 time steps). Residential load profiles for typical mid-week, winter scenarios were generated based on the associated PDFs.

Fig. 16 shows the distribution of measured voltages for all CPOCs over all charging periods for the scenario with no EVs on the network and the scenario with 50% EV penetration with optimized vehicle charging. This graph shows that the majority of pre-optimization voltage measurements are near or above 1 pu with reduced occurrences for decreasing voltage levels. Following the application of the optimization technique, the majority of voltage measurements are recorded between 0.91 and 0.95 pu indicating that the optimization technique was able to maintain CPOC voltages above the low voltage limit for the network. Any occurrence of voltage levels below the lower voltage limit, in both the case with no EVs and the optimized case, is due to the household demand. As a result, these voltages remain unaffected in the optimized case as the technique does not allow EV charging if the network is already exceeding limits.

The distribution of thermal loading results for the transformer during the analysis is presented in Fig. 17. Prior to the addition of EVs, the majority of loading measurements were found to lie

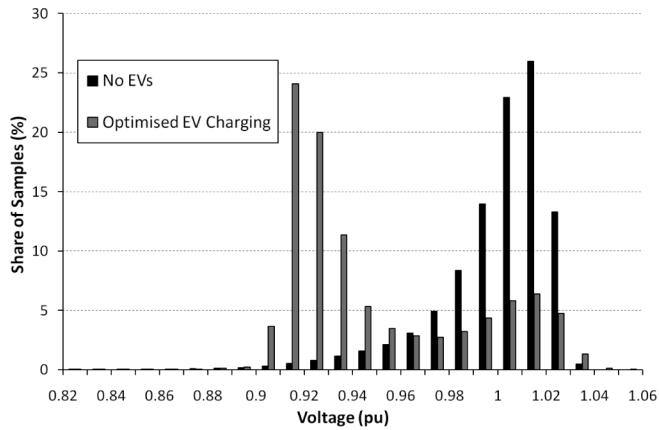


Fig. 16. Distribution of measured voltages at network CPOCs.

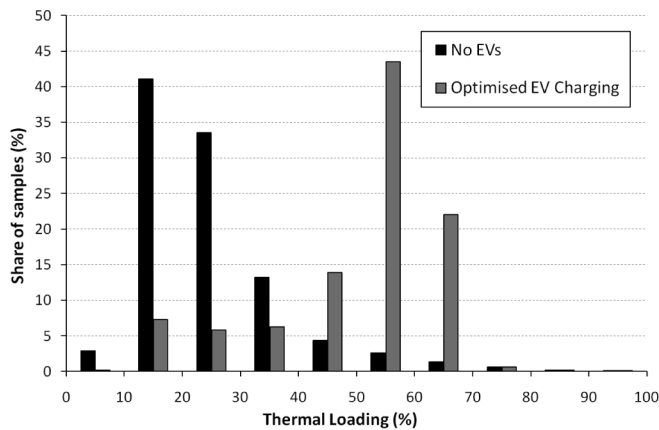


Fig. 17. Distribution of measured thermal loading levels for the network transformer.

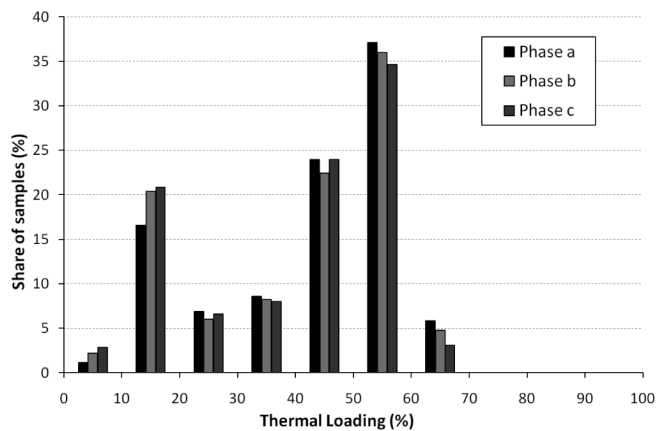


Fig. 18. Distribution of measured loading levels on each phase of the three-phase mains cable supplying the network from the transformer (optimized EV charging).

between 10% and 30% of rated loading. Following the introduction of EVs, charged according to the optimization method, the majority of recorded measurements were found to be in the region of 50%–70% of rated loading.

Fig. 18 shows the distribution of measured thermal loading for each phase of the three-phase mains cable supplying the feeder from the LV transformer. These measurements are from

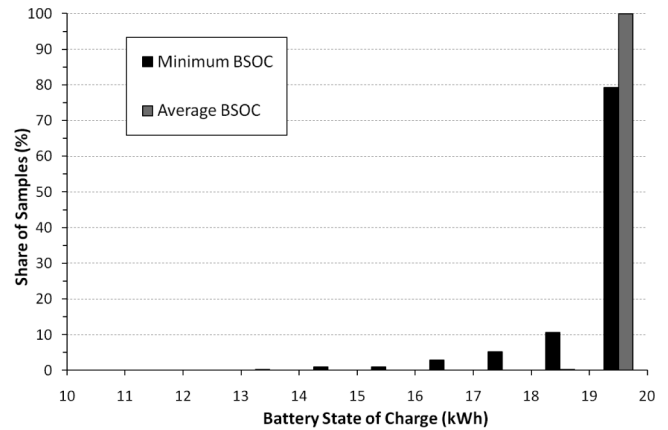


Fig. 19. Distribution of minimum and average BSOCs for all EVs recorded at the end of each charging period.

the optimized case only. As can be seen from the loading results for both the transformer and the mains cable, the rated loading limit for either component is never the constraining factor for the optimization method. It is apparent that, for this particular network, the electrical components are more than adequately rated to accept the increased loading due to a high penetration of charging EVs. Instead, the voltage limits are more likely to be an issue with off-peak EV charging and, as a result, are typically the constraining factor in the optimization method.

Fig. 19 shows results for the final BSOC of all EVs after each charging period, representing the BSOC of the EV with the least BSOC, as well as the average BSOC of all EVs. For the high penetration level of charging EVs examined, the optimization technique results in an average BSOC of 99.9%. While it is possible that not every EV will have a full BSOC by the end of the charging period, such cases occur far less frequently. The lowest final BSOC recorded over the analysis was 13.3 kWh (66.5%).

The average losses on the LV feeder over all charging periods were found to be 11 kWh for the case with no EVs and 80 kWh for the optimized charging case using the weighted objective function method.

## V. CONCLUSION

The introduction of large penetrations of EVs will have significant impacts on the operating conditions of distribution networks. If they are to be charged in a passive, uncontrolled manner, then major infrastructure upgrades may be required. Controlled charging by the DSO could help to alleviate some of these issues and allow EV owners to charge their vehicles while maintaining the network within acceptable operating limits. The work presented here has demonstrated how the charging rates of a high penetration of EVs on a test network can be optimized in order to deliver the maximum amount of energy to the EVs within a set charging period subject to network constraints, while ensuring that the underlying residential load remains unaffected.

Results from this work have shown that maximizing the total power to all EVs according to network constraints will favor those EVs that are connected near to the transformer, rather than those connected towards the extremes of the radial network.

TABLE III  
CABLE CHARACTERISTICS

Line	Length (m)	$R_1$ ( $\Omega$ )	$X_1$ ( $\Omega$ )	$R_0$ ( $\Omega$ )	$X_0$ ( $\Omega$ )	C ( $\mu F$ )	$I_{rated}$ (A)
MV	10,000	20.8	4	10	12	0.01	1000
1-2	190	0.032	0.014	0.095	0.041	0.053	510
2-3	27.5	0.008	0.002	0.024	0.006	0.008	368
3-4	85	0.024	0.006	0.073	0.018	0.026	368
4-5	97.5	0.028	0.007	0.084	0.021	0.029	368
5-6	154	0.062	0.011	0.185	0.033	0.046	300
4-7	119	0.048	0.009	0.143	0.026	0.036	300
2-8	32.5	0.009	0.002	0.028	0.007	0.01	368
8-9	59	0.017	0.004	0.051	0.013	0.018	368
9-10	106	0.03	0.008	0.091	0.023	0.032	368
10-11	95	0.027	0.007	0.082	0.021	0.029	368
9-12	217.5	0.087	0.016	0.261	0.047	0.065	368
Service Cable (per km)		0.8	0.07	-	-	0.4	80

$R_1$  Positive sequence resistance       $R_0$  Zero sequence resistance  
 $X_1$  Positive sequence reactance       $X_0$  Zero sequence reactance  
C Capacitance       $I_{rated}$  Rated current

Therefore, a weighted objective function was studied, which optimized the EV charging rates according to both the impact on the network operating conditions and the BSOC of the EVs. Results show that the modified objective function increases the total energy delivered to the EVs. This objective function was also tested for various charging period scenarios and was shown to return an average BSOC of 99.9% for all EVs over all periods examined.

Due to the use of linear programming, large amounts of data are not required by the DSO at each time step in order to find the optimal rate of charge for each EV. The technique is not computationally intense nor does it require storage of historical load data for subsequent use, and therefore could be easily incorporated into a coordinated charging scheme. Determining the various network sensitivities to additional load provides insight into the condition of the network and could prove very useful for DSOs employing such schemes. Assuming the use of AMI within residential households and sufficient communication links between the DSO and the AMI metering, practical implementation of the optimal charging method would provide significant benefits in terms of accommodating high penetrations of EVs.

#### APPENDIX

Table III shows the cable characteristics.

#### ACKNOWLEDGMENT

The authors would like to acknowledge ESB Networks for providing the necessary data for carrying out this work.

#### REFERENCES

- [1] Smarter Travel, a Sustainable Transport Future: A New Transport Policy for Ireland 2009–2020, Department of Transport, Ireland, 2009. [Online]. Available: <http://www.transport.ieuploadgeneral112840.pdf>.

- [2] Ultra-Low Carbon Cars: Next Steps on Delivering the £250 Million Consumer Incentive Programme for Electric and Plug-in Hybrid Cars, Department for Transport, U.K., 2009. [Online]. Available: <http://www.dft.gov.ukadobepdf163944ulcc.pdf>.
- [3] J. Heywood, P. Baptista, I. Berry, K. Bhatt, L. Cheah, F. de Sisternes, V. Karplus, D. Keith, M. Khushid, D. MacKenzie, and J. McAulay, An Action Plan for Cars: The Policies Needed to Reduce U.S. Petroleum Consumption and Greenhouse Gas Emissions, Massachusetts Institute of Technology Energy Initiative Report, 2009. [Online]. Available: [http://web.mit.edu/sloan-auto-lab/research/beforeh2/actionplan/ActionPlan\\_CombinedFinal\\_ForPublication\\_8Feb10.pdf](http://web.mit.edu/sloan-auto-lab/research/beforeh2/actionplan/ActionPlan_CombinedFinal_ForPublication_8Feb10.pdf).
- [4] G. T. Heydt, "The impact of electric vehicle deployment on load management strategies," *IEEE Trans. Power App. Syst.*, vol. PAS-102, no. 5, pp. 1253–1259, May 1983.
- [5] S. Rahman and G. B. Shrestha, "An investigation into the impact of electric vehicle load on the electric utility distribution system," *IEEE Trans. Power Del.*, vol. 8, no. 2, pp. 591–597, Apr. 1993.
- [6] J. Taylor, A. Maitra, M. Alexander, D. Brooks, and M. Duvall, "Evaluation of the impact of plug-in electric vehicle loading on distribution system operations," in *Proc. IEEE Power and Energy Soc. General Meeting*, Calgary, AB, Canada, Jul. 2009.
- [7] K. Schneider, C. Gerkensmeyer, M. Kintner-Meyer, and R. Fletcher, "Impact assessment of plug-in hybrid vehicles on Pacific Northwest distribution systems," in *Proc. IEEE Power and Energy Soc. General Meeting*, Pittsburgh, PA, Jul. 2008.
- [8] C. Gerkensmeyer, M. Kintner-Meyer, and J. G. DeSteele, Technical Challenges of Plug-in Hybrid Electric Vehicles and Impacts to the US Power System: Distribution System Analysis, Pacific Northwest National Laboratory Report, 2010. [Online]. Available: [http://www.pnl.gov/main/publications/external/technical\\_reports/PNNL-19165.pdf](http://www.pnl.gov/main/publications/external/technical_reports/PNNL-19165.pdf).
- [9] S. Shao, M. Pipattanasomporn, and S. Rahman, "Challenges of PHEV penetration to the residential distribution network," in *Proc. IEEE Power and Energy Soc. General Meeting*, Calgary, AB, Canada, Jul. 2009.
- [10] G. A. Putrus, P. Suwanapongkarl, D. Johnston, E. C. Bentley, and M. Narayana, "Impact of electric vehicles on power distribution networks," in *Proc. IEEE Vehicle Power and Propulsion Conf.*, Dearborn, MI, Sep. 2009.
- [11] P. Richardson, D. Flynn, and A. Keane, "Impact assessment of varying penetrations of electric vehicles on low voltage distribution systems," in *Proc. IEEE Power and Energy Soc. General Meeting*, Minneapolis, MN, Jul. 2010.
- [12] J. A. P. Lopes, S. A. Polenz, C. L. Moreira, and R. Cherkaoui, "Identification of control and management strategies for LV unbalanced microgrids with plugged-in electric vehicles," *J. Elect. Power Syst. Res.*, vol. 80, no. 8, pp. 898–906, Aug. 2010.
- [13] S. Acha, T. C. Green, and N. Shah, "Effects of optimised plug-in hybrid vehicle charging strategies on electric distribution network losses," in *Proc. IEEE Power and Energy Soc. Transmission and Distribution Conf. Expo.*, New Orleans, LA, Apr. 2010.
- [14] K. Clement, E. Haesen, and J. Driesen, "The impact of charging plug-in hybrid electric vehicles on a residential distribution grid," *IEEE Trans. Power Syst.*, vol. 25, no. 1, pp. 371–380, Feb. 2010.
- [15] K. Clement-Nyngs, E. Haesen, and J. Driesen, "Analysis of the impact of plug-in hybrid electric vehicles on residential distribution grids by using quadratic and dynamic programming," in *Proc. EVS24 International Battery, Hybrid and Fuel Cell Electric Vehicle Symp.*, Stavanger, Norway, May 2009.
- [16] A. Brooks, E. Lu, D. Reicher, C. Spirakis, and B. Wehl, "Demand dispatch: Using real-time control of demand to help balance generation and load," *IEEE Power Energy Mag.*, vol. 8, no. 3, pp. 20–29, May/Jun. 2010.
- [17] E. Sortomme and M. A. El-Sharkawi, "Optimal charging strategies for unidirectional vehicle-to-Grid," *IEEE Trans. Smart Grid*, vol. 2, no. 1, pp. 131–138, Mar. 2011.
- [18] F. Hoffart, "Proper care extends Li-ion battery life," *Power Electron. Technol.*, Apr. 2008. [Online]. Available: [http://powerelectronics.com/portable\\_power\\_management/battery\\_charger\\_ics/proper\\_care\\_extends-li-ion-battery-0425/index.html](http://powerelectronics.com/portable_power_management/battery_charger_ics/proper_care_extends-li-ion-battery-0425/index.html).
- [19] DiGSILENT PowerFactory. DiGSILENT GmbH. [Online]. Available: <http://www.digsilent.de/>.
- [20] MATLAB R2009a, The MathWorks, Inc..
- [21] ESB Networks Distribution Code, 2007. [Online]. Available: <http://www.esb.ie/esbnetworks/en/downloads/Distribution-Code.pdf>.
- [22] W. H. Kersting, *Distribution System Modeling and Analysis*. London, U.K.: CRC, 2002.
- [23] H. L. Willis, *Power Distribution Planning Reference Book*. Basel, Switzerland: Marcel Dekker, 2004.
- [24] *IEEE Guide for Loading Mineral-Oil-Immersed Transformers*, IEEE Std. C57.91, 1995.



**Peter Richardson** (S'08) received the B.E. degree in electrical engineering from University College Dublin, Dublin, Ireland, in 2007, where he is currently pursuing the Ph.D. degree.

His research interests are in electric vehicles, distributed energy resources, and distribution networks.



**Andrew Keane** (S'04–M'07) received the B.E. and Ph.D. degrees in electrical engineering from University College Dublin, Dublin, Ireland, in 2003 and 2007, respectively.

He is currently a lecturer with the School of Electrical, Electronic, and Mechanical Engineering, University College Dublin with research interests in power systems planning and operation, distributed energy resources, and distribution networks.



**Damian Flynn** (M'96) is a senior lecturer in power engineering at University College Dublin, Dublin, Ireland. His research interests involve an investigation of the effects of embedded generation sources, especially renewables, on the operation of power systems. He is also interested in advanced modeling and control techniques applied to power plant.